

1996

# Evolution of a forearc basin in arc-continent collision, offshore Taiwan

Justin Owen Hirtzel  
*San Jose State University*

Follow this and additional works at: [https://scholarworks.sjsu.edu/etd\\_theses](https://scholarworks.sjsu.edu/etd_theses)

---

## Recommended Citation

Hirtzel, Justin Owen, "Evolution of a forearc basin in arc-continent collision, offshore Taiwan" (1996). *Master's Theses*. 1286.  
DOI: <https://doi.org/10.31979/etd.9ya9-8bg8>  
[https://scholarworks.sjsu.edu/etd\\_theses/1286](https://scholarworks.sjsu.edu/etd_theses/1286)

This Thesis is brought to you for free and open access by the Master's Theses and Graduate Research at SJSU ScholarWorks. It has been accepted for inclusion in Master's Theses by an authorized administrator of SJSU ScholarWorks. For more information, please contact [scholarworks@sjsu.edu](mailto:scholarworks@sjsu.edu).

## INFORMATION TO USERS

This manuscript has been reproduced from the microfilm master. UMI films the text directly from the original or copy submitted. Thus, some thesis and dissertation copies are in typewriter face, while others may be from any type of computer printer.

**The quality of this reproduction is dependent upon the quality of the copy submitted.** Broken or indistinct print, colored or poor quality illustrations and photographs, print bleedthrough, substandard margins, and improper alignment can adversely affect reproduction.

In the unlikely event that the author did not send UMI a complete manuscript and there are missing pages, these will be noted. Also, if unauthorized copyright material had to be removed, a note will indicate the deletion.

Oversize materials (e.g., maps, drawings, charts) are reproduced by sectioning the original, beginning at the upper left-hand corner and continuing from left to right in equal sections with small overlaps. Each original is also photographed in one exposure and is included in reduced form at the back of the book.

Photographs included in the original manuscript have been reproduced xerographically in this copy. Higher quality 6" x 9" black and white photographic prints are available for any photographs or illustrations appearing in this copy for an additional charge. Contact UMI directly to order.

# UMI

A Bell & Howell Information Company  
300 North Zeeb Road, Ann Arbor MI 48106-1346 USA  
313/761-4700 800/521-0600



**EVOLUTION OF A FOREARC BASIN  
IN ARC-CONTINENT COLLISION,  
OFFSHORE TAIWAN**

**A Thesis**

**Presented to**

**The Faculty of the Department of Geology**

**San Jose State University**

**In Partial Fulfillment**

**of the Requirements for the Degree**

**Master of Science**

**By**

**Justin Owen Hirtzel**

**August, 1996**

**UMI Number: 1381313**

---

**UMI Microform 1381313  
Copyright 1996, by UMI Company. All rights reserved.**

**This microform edition is protected against unauthorized  
copying under Title 17, United States Code.**

---

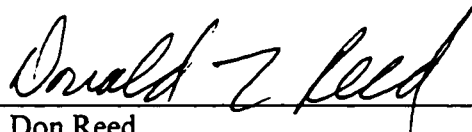
**UMI**  
300 North Zeeb Road  
Ann Arbor, MI 48103

© 1996

Justin Owen Hirtzel

**ALL RIGHTS RESERVED**

APPROVED FOR THE DEPARTMENT OF GEOLOGY



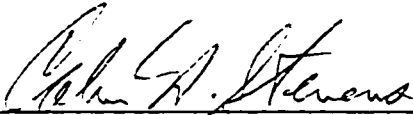
---

Dr. Don Reed



---

Dr. Richard Sedlock



---

Dr. Calvin Stevens

APPROVED FOR THE UNIVERSITY



## ABSTRACT

### FOREARC BASIN EVOLUTION IN ARC-CONTINENT COLLISION, OFFSHORE TAIWAN

by Justin O. Hirtzel

The North Luzon trough is a forearc basin extending from the subduction zone to the arc-continent collision zone, south of Taiwan. Seismic stratigraphic analysis of forearc basin sediments, combined with studies of recent sedimentation processes using *SeaMARC II* swath-mapping, is used to examine the evolution of this region. These sediments were derived from the volcanic arc and deposited by sediment-gravity flows and through mass wasting along the rear of the accretionary prism. Detritus from the Taiwan mountain belt is trapped in a series of satellite basins to the north of the forearc basin or directed into the backarc region as a result of seafloor deformation along the active collision suture. A decrease in thickness of the upper three seismic sequences along the western margin of the basin marks the onset of uplift of basin strata due to tectonic wedging along the rear of the accretionary prism.



## ACKNOWLEDGMENTS

I thank Dr. Don Reed for his guidance and input on this project. I also owe a debt of gratitude to him for sharing his knowledge of science, and a home cooked Thanksgiving dinner. My appreciation also goes to Drs. Richard Sedlock and Calvin Stevens for their participation on my committee. I would like to thank the faculty and staff of the Department of Geology for providing an environment conducive to both scholastic and personal growth. Special thanks to D. Fox and Alfonse for providing technical support above and beyond the call of duty. Thanks also to Jade for putting up with cross-country requests and just being a pal. I would also like to thank Wu-Cheng and Ching-Yen (my two favorite people from Taiwan), Erick and Angela (a.k.a. The Sunnyvale Bed and Breakfast), Lewis, Marc, and Doo Sung Yi for their support and friendship.

My thanks also goes to the faculty and staff of the Marine Science Department at Coastal Carolina University, especially Dr. Paul T. Gayes who sparked my interest in Geology and Geophysics and is partly responsible for where I am today.

Last but not least, my thanks goes to my family whose love and support has followed me across the country and around the world. This I cherish the most and am forever grateful!

## TABLE OF CONTENTS

	Page
ABSTRACT.....	vii
INTRODUCTION.....	1
TECTONIC SETTING.....	3
DATA ACQUISITION AND PROCESSING.....	11
Acquisition.....	11
Processing.....	11
DATA ANALYSIS.....	16
Seismic Stratigraphy.....	16
Definition and Guidelines.....	16
Geometry and Distribution of Sequences.....	17
Sedimentary Processes.....	24
INTERPRETATIONS.....	26
Seismic Stratigraphy.....	26
Sedimentary Processes.....	31
CONCLUSIONS.....	38
REFERENCES.....	39

## LIST OF FIGURES

	Page
Figure 1. Three-Dimensional Illustration Showing Taiwan's Tectonic Setting.....	4
Figure 2. Location Map of Features Associated with Taiwan Arc-Continent Collision.....	5
Figure 3. Map Showing Rates of Convergence.....	6
Figure 4. Evolution of Arc-Continent Collision.....	8
Figure 5. Map Showing the Three Main Structural Domains.....	9
Figure 6. Cross-Sections of Taiwan's Offshore Accretionary Prism.....	10
Figure 7. Map Showing Ship Track Lines.....	12
Figure 8. Portion of Side-Scan Sonar Image Mosaic.....	13
Figure 9. Map Showing <i>SeaMARC II</i> Bathymetric Data.....	14
Figure 10. Seismic Data Processing Flow.....	15
Figure 11. Isochron Map of Forearc Basin Sediment Thickness.....	18
Figure 12. Cross-Section of Forearc Basin Sediments.....	19
Figure 13. Cross-Section of the Forearc Basin Illustrating Broad Anticlines.....	23
Figure 14. Model Illustrating the Eastward Progression of the Tectonic Wedge.....	28
Figure 15. Two-Way Travel Time Contour Map.....	30
Figure 16. Side-Scan Sonar Interpretation.....	32
Figure 17. Contour Map Showing the Submarine Canyon North of the Forearc Basin.....	34
Figure 18. Drawing of Line 20 Showing Evidence for Debris-Flow Deposits.....	35
Figure 19. Model Showing Progressive Forms of Mass Wasting.....	37

## ABSTRACT

The North Luzon trough is a forearc basin extending from the subduction zone to the arc-continent collision zone, south of Taiwan. Seismic stratigraphic analysis of forearc basin sediments, combined with studies of recent sedimentation processes using *SeaMARC II* swath-mapping, is used to examine the evolution of this region. Layered sediments within the trough reach a maximum thickness of 4.0 sec (two-way travel time) in the region of subduction and decrease in thickness northward towards the region of arc-continent collision. Nine seismic sequences, which consist of sheet and wedge-shaped bodies that onlap the arc basement, are recognized in the basin. These sediments were deposited by sediment-gravity flows from the volcanic arc and the Taiwan orogen. Sediments were also transported to the basin by mass wasting along the rear of the accretionary prism. Basin-wide unconformities are not identified between these sequences in the central and eastern regions of the basin, suggesting relatively continuous sedimentation and the absence of significant tilting of the underlying arc basement despite the onset of collision and closure of the forearc basin. Detritus from the Taiwan mountain belt is currently trapped in a series of satellite basins to the north of the forearc basin or directed into the backarc region as a result of seafloor deformation along the active collision suture. A decrease in thickness of the upper three seismic sequences along the western margin of the basin marks the onset of uplift of basin strata due to tectonic wedging along the rear of the accretionary prism as a result of arc-continent collision.

## INTRODUCTION

Seismic sequence analysis can be used to study tectonic processes in the vicinity of sedimentary basins. For example, stratigraphic sequences in piggyback basins have been used to investigate thrust movement in Argentina and northern Italy (Beer et al., 1990; Ori and Friend, 1984), thrust loading resulting in subsidence has been examined in collisional basin settings (Lundberg and Dorsey, 1988), and tectonic wedging has been studied in ancient and modern forearc settings (Price, 1986; Silver and Reed, 1988; Torrini and Speed, 1989; Speed et al., 1989; Unruh et al., 1991). In addition, a better understanding of forearc evolution has been provided through seismic stratigraphic analyses by Lewis and Hayes (1984) and Beaudry and Moore (1985).

The main goal of this study was to gain insight into the evolution of the North Luzon trough, a forearc basin extending across the transition from subduction to arc-continent collision south of Taiwan. This study examines the evolution of this region through a seismic stratigraphic analysis of migrated seismic profiles and observations made from *SeaMARC II* swath-mapping data. Nine seismic sequences are recognized throughout the basin, and isochron maps were generated for sequence thickness and depth to each sequence boundary. In addition, isochron maps were generated for the total sediment thickness and depth to the volcanic-arc basement. In general, these maps show a southwestward increase in sediment thickness and depth to basement. The three-dimensional shape of the sequences can be described as sheet drape to slightly wedge-

shaped deposits that lap onto the volcanic-arc basement to the east. Small deep-sea fan deposits are of local importance, especially near the volcanic arc.

One important finding of the study is that the boundary between sequences 3 and 4 marks the relative timing for the onset of uplift of basin sediments along the western border of the North Luzon trough. Uplift of the sequences is primarily due to backthrusting and tectonic wedging along the rear of the accretionary prism.

Another important result of the study is that backthrusting and tectonic wedging in this region causes the incorporation of forearc basin strata into the rear of the accretionary prism in the region of incipient collision. These strata are uplifted, subjected to processes of mass wasting, and redeposited in the forearc basin. Forearc basin strata in this region may experience several cycles of uplift, mass failure, and redeposition in the trough prior to the impingement of the Luzon volcanic arc onto the rear of the accretionary prism. To the north, where the arc is being accreted to the Chinese continental margin, the forearc basin is segmented into several satellite basins that serve as traps for detritus shed from the Taiwan orogen.

## TECTONIC SETTING

The island of Taiwan is located in the South China Sea along the boundary of the Eurasian and Philippine Sea plates. This boundary is one of oblique plate convergence, which exhibits components of subduction and arc-continent collision along a contiguous forearc system. South of Taiwan the Eurasian plate is subducting eastward beneath the Philippine Sea plate along the Manila trench, whereas to the north of the island, the Philippine Sea plate is being subducted beneath the Eurasian plate along the Ryukyu trench (Fig. 1).

Subduction south of Taiwan has formed the Manila trench, the Taiwan accretionary prism, the North Luzon trough, and the Luzon volcanic arc (Fig. 2). Between the latitudes of  $21^{\circ} 30' N$  and  $22^{\circ} 00' N$ , the Chinese continental margin enters the subduction zone marking the onset of arc-continent collision (Reed et al., 1992). The timing of this collision is not fully constrained, but it has been proposed to have begun in the middle Miocene in the vicinity of northern Taiwan and propagated southward at a rate of approximately 80-90 km/my (Suppe, 1984; Teng, 1991) (Fig. 3). Thus, observations of the area 80-90 km south of the present collision point are analogous to viewing the present collision as it was approximately one million years ago. This relationship is evident in general observations of the decreasing width of the North Luzon trough northward towards the point of collision, which is accompanied by the increasing width and uplift of the accretionary prism.

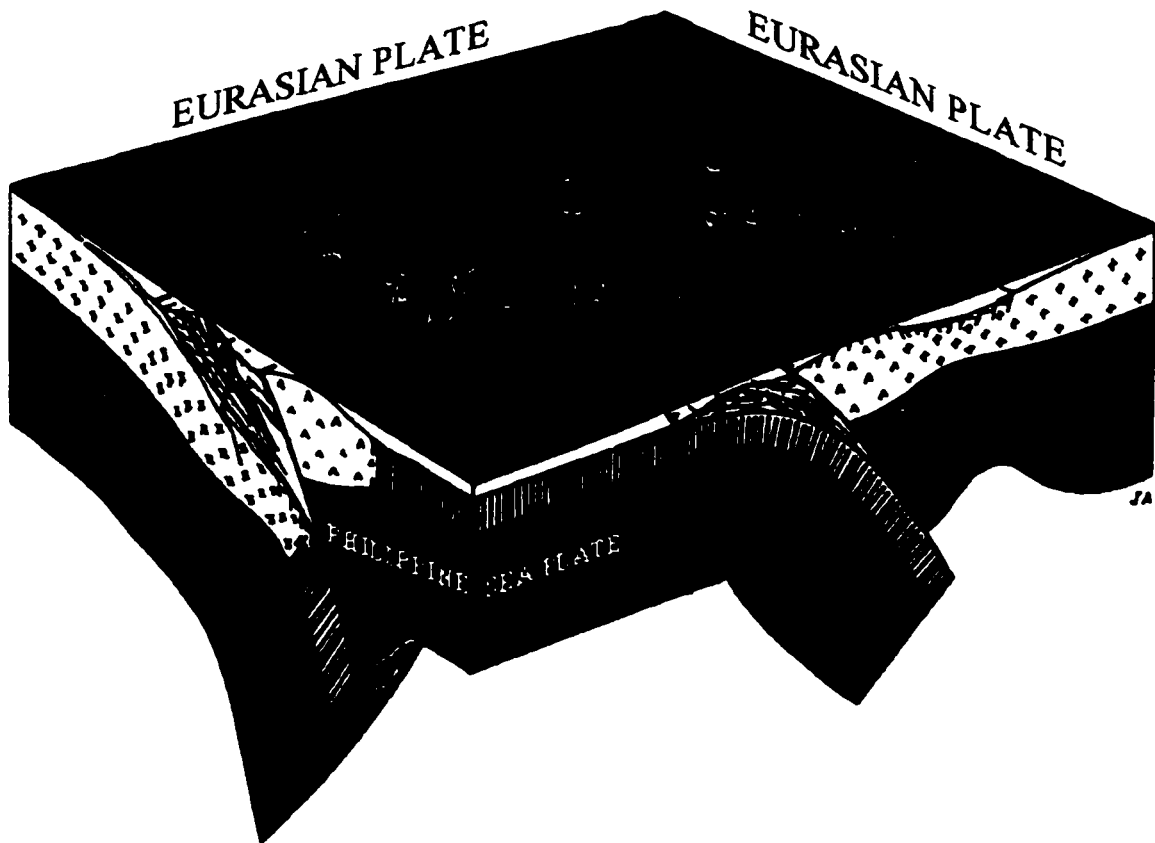


Figure 1. Three-dimensional illustration showing Taiwan's tectonic setting (modified from Angelier et al., 1990).



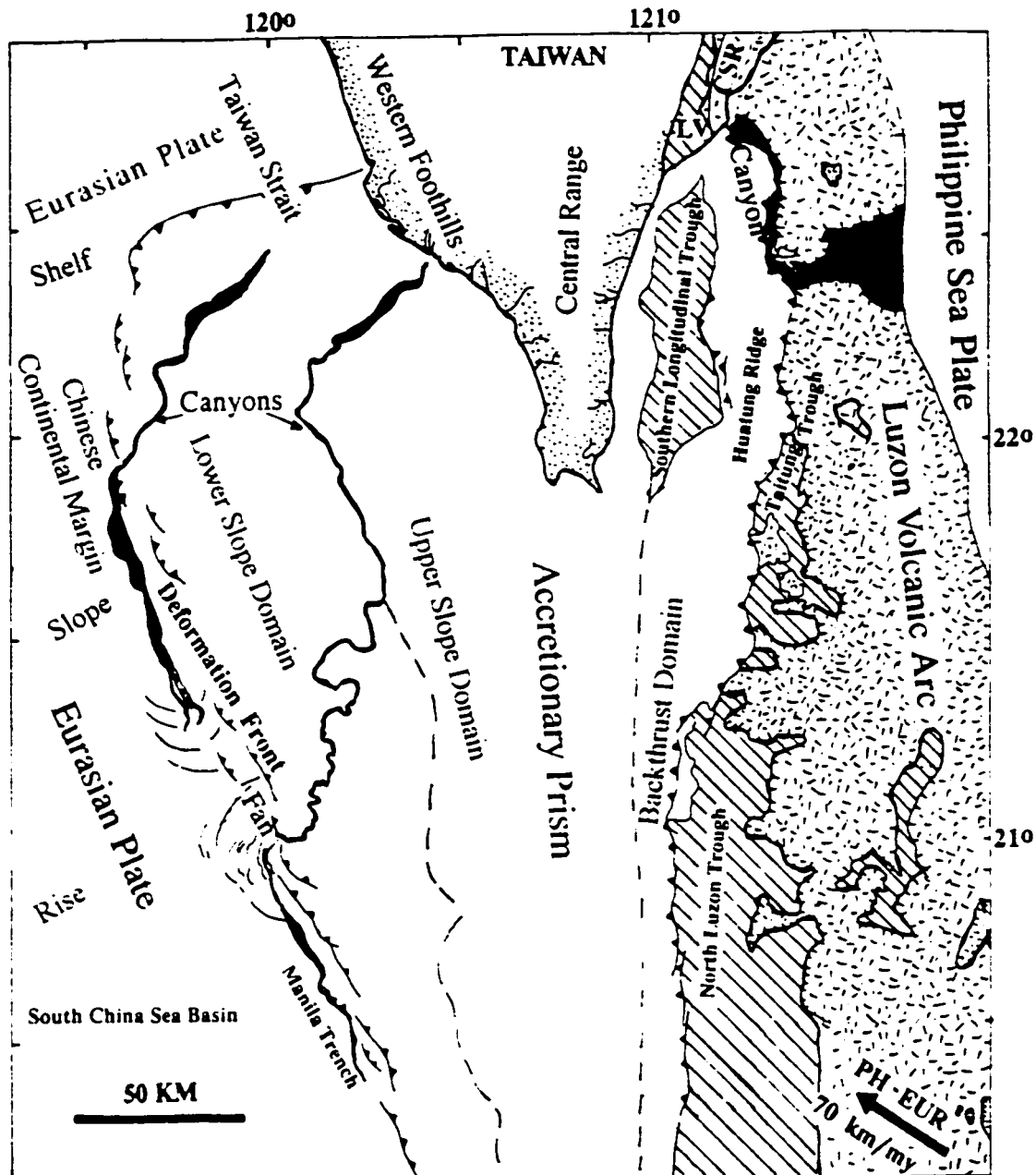


Figure 2 Location map of features associated with the Taiwan arc-continent collision (modified from Reed et al., 1992). Motion of the Philippine Sea plate with respect to the Eurasian plate (PH-EUR) is from Seno (1977). Dashed lines depict boundaries between the lower slope, upper slope, and backthrust domains of the accretionary prism. Locations of major basinal deposits, including the modern forearc basin represented by the North Luzon trough are shown by diagonal lines. Prominent submarine canyons are shown in black. Symbols: LV - Longitudinal Valley. CSR - Coastal Range.

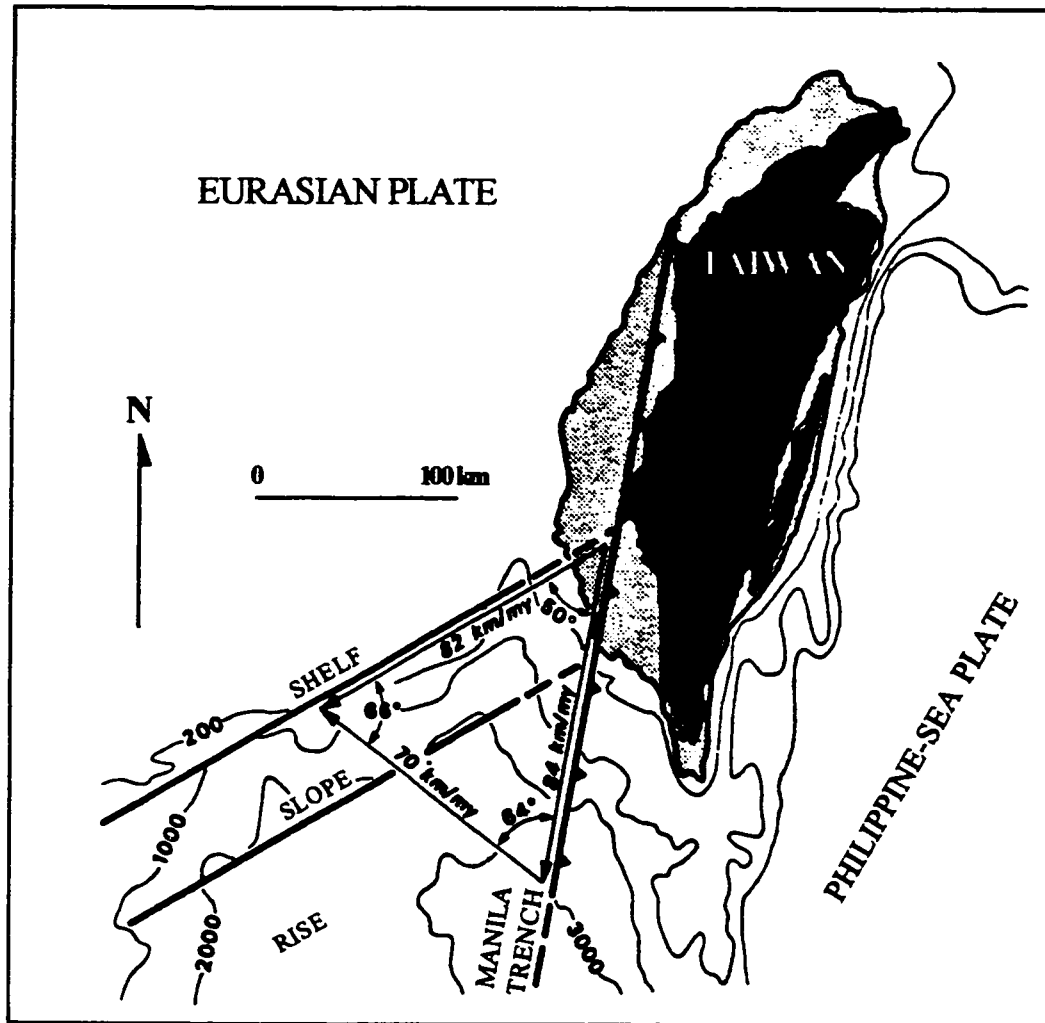


Figure 3. Map showing rates of convergence and proposed rate of collision propagation southward along the Manila trench (modified from Suppe, 1984).

The evolution of the arc-continent collision, as proposed by Teng (1991), is shown in Figure 4. This figure illustrates the development of the forearc basin and the eventual incorporation of its sediments into what is now the Central Range and Coastal Range on land.

Reed and others (1992) divided the Taiwan offshore accretionary prism into three main structural domains (Fig. 5): (1) a lower slope domain, characterized by moderate deformation and mainly west-vergent thrust faults; (2) an upper slope domain, characterized by intense deformation; and (3) a backthrust domain distinguished by thrust deformation along the rear of the prism. Cross-sections of the offshore accretionary prism (Fig. 6) show changes in the overall geometry of the North Luzon trough from the zone of subduction in the south to the zone of incipient collision in the north, where east-directed backthrusts underlie anticlines in forearc basin strata. Convergence along the rear of the accretionary prism results in the deformation and uplift of the entire forearc basin sequence, creating the Huatang ridge (Fig. 2). This ridge forms a bathymetric high in the submarine environment that serves as a trap for detritus derived from southeastern Taiwan. Modern detritus from the Taiwan orogen is deposited in the form of basin-fill sequences in the Southern Longitudinal trough (Fig. 5), the offshore extension of Taiwan's Longitudinal valley, which has been identified as the suture between the Luzon arc and the Chinese continental margin (Teng, 1991).

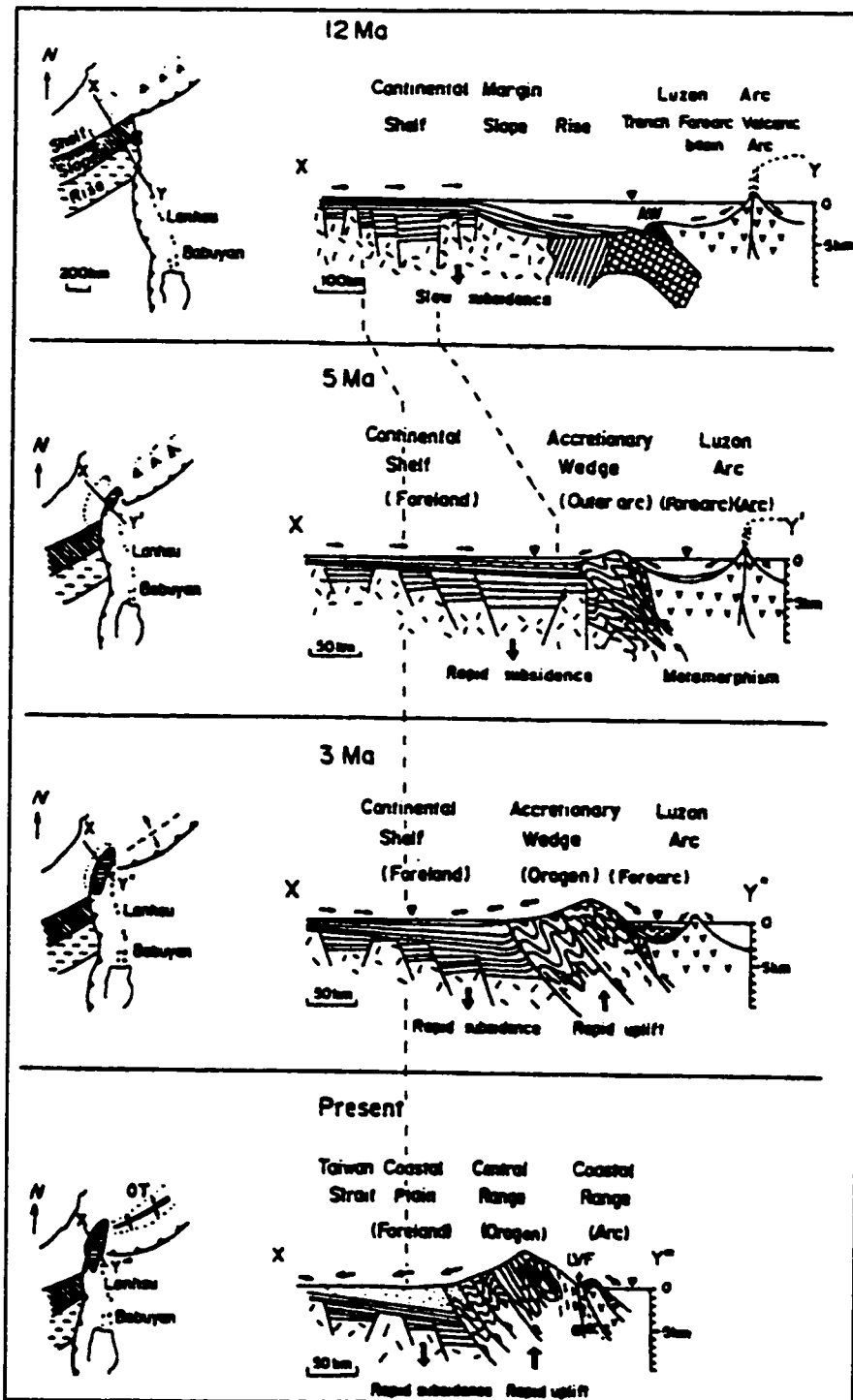


Figure 4. Evolution of arc-continent collision (modified from Teng, 1991). Symbols of provinces: AW - Accretionary Wedge, OT - Okinawa Trough, and LVF - Longitudinal Valley Fault

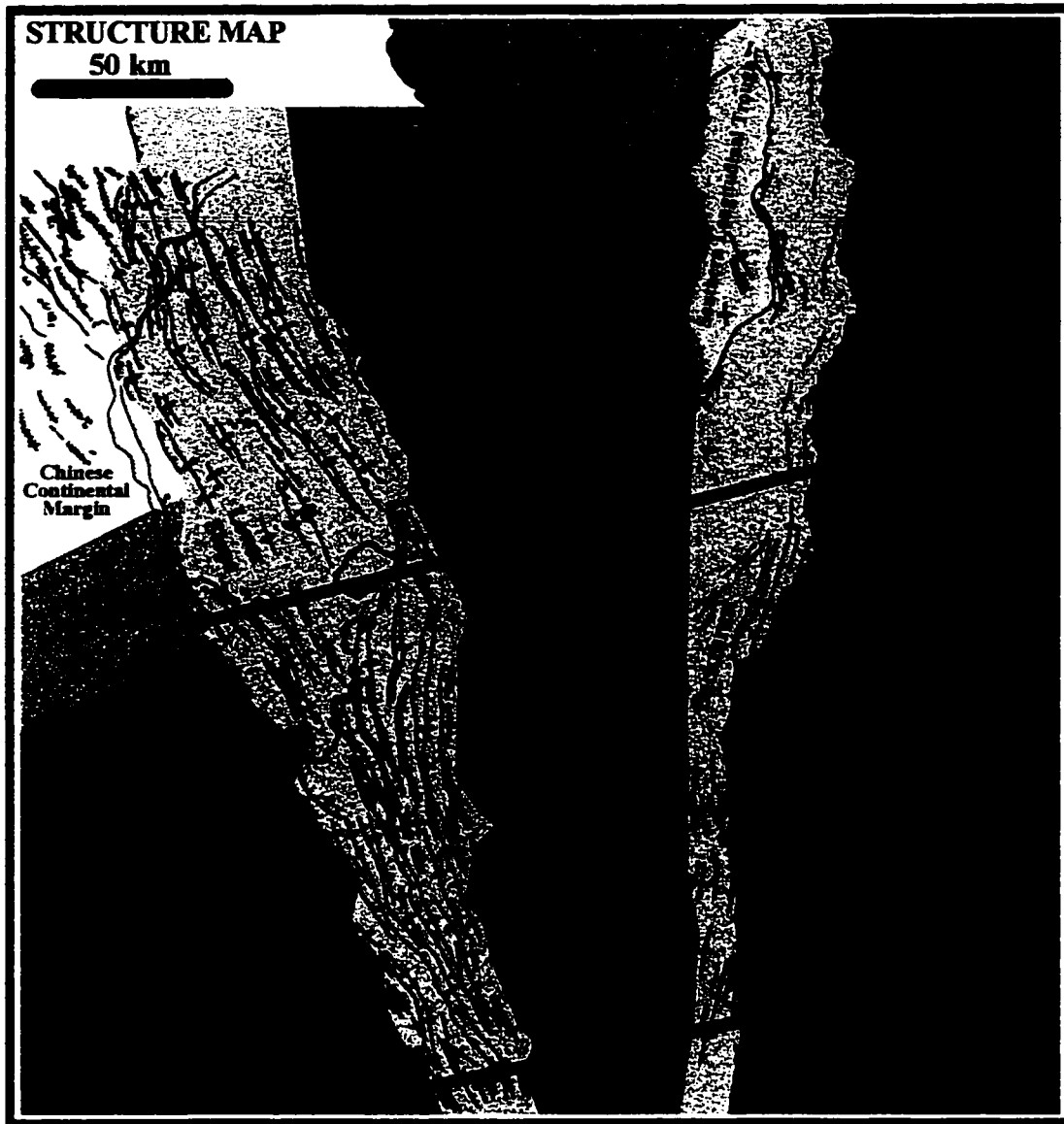


Figure 5. Map showing the three main structural domains and their relation to subduction and arc-continent collision offshore Taiwan (modified from Reed et al., 1992). Cross-sections A - A' and B - B' shown in Figure 6.

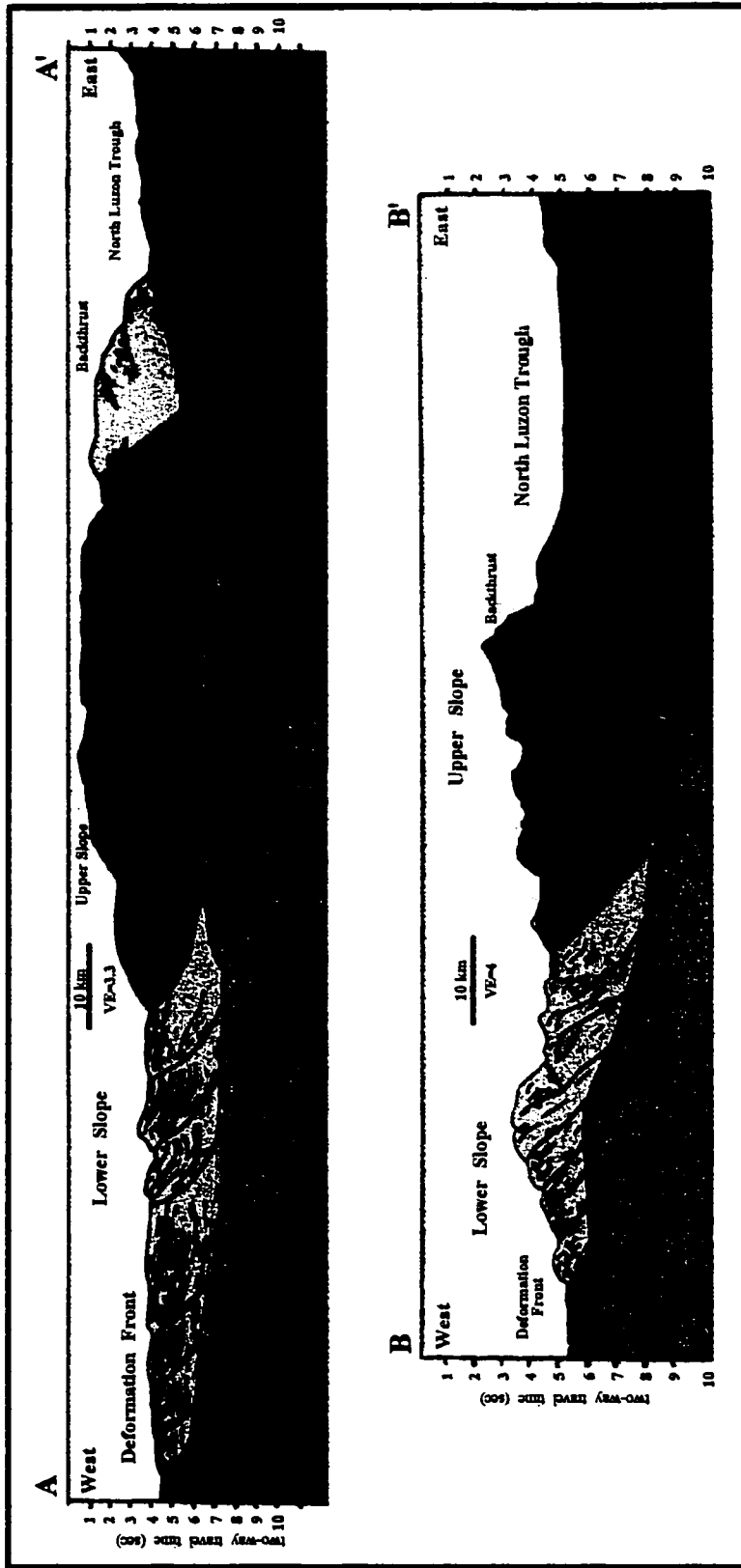


Figure 6. Cross-sections of Taiwan's offshore accretionary prism illustrating wedge geometry in regions of arc-continent collision (top) and subduction (bottom) (modified from Reed et al., 1992). For locations of cross-sections, and color coding see Figure 5.

## DATA ACQUISITION AND PROCESSING

### Acquisition

This study is based on a suite of geophysical data collected in May and June of 1990 aboard the R/V *Moana Wave* of the University of Hawaii. Figure 7 shows a map of the survey area with the main focus for this study outlined in white. The data coverage spans an area from the Manila trench in the west to the Luzon island arc in the east, consisting of >50,000 km<sup>2</sup> of *SeaMARC II* side-scan sonar and bathymetry data and >8,000 line km of 6-channel seismic reflection data. In addition, 3.5 kHz echo profiling, gravity, and magnetic data were collected along each line.

The seismic data were acquired using a 2-gun (460 in<sup>3</sup>) array source and a 6-channel receiver with 25 m sections. A 37.5 m shot interval was used to produce a 4-fold CDP spaced at 25 m with an average line spacing of approximately 8 km.

### Processing

Mosaics of the *SeaMARC II* side-scan sonar and bathymetry data were constructed by members of the initial survey team (Figs. 8 & 9 respectively). All but two lines of the seismic data were processed at University of California, Santa Cruz utilizing the processing software, *SIOSEIS*. Two strike lines running roughly north-south along the axis of the forearc basin were processed by the author on the *SPARC* station 10 in the Department of Geology at San Jose State University using *SIOSEIS*. Figure 10 shows the data processing flow used at both UC Santa Cruz and SJSU.

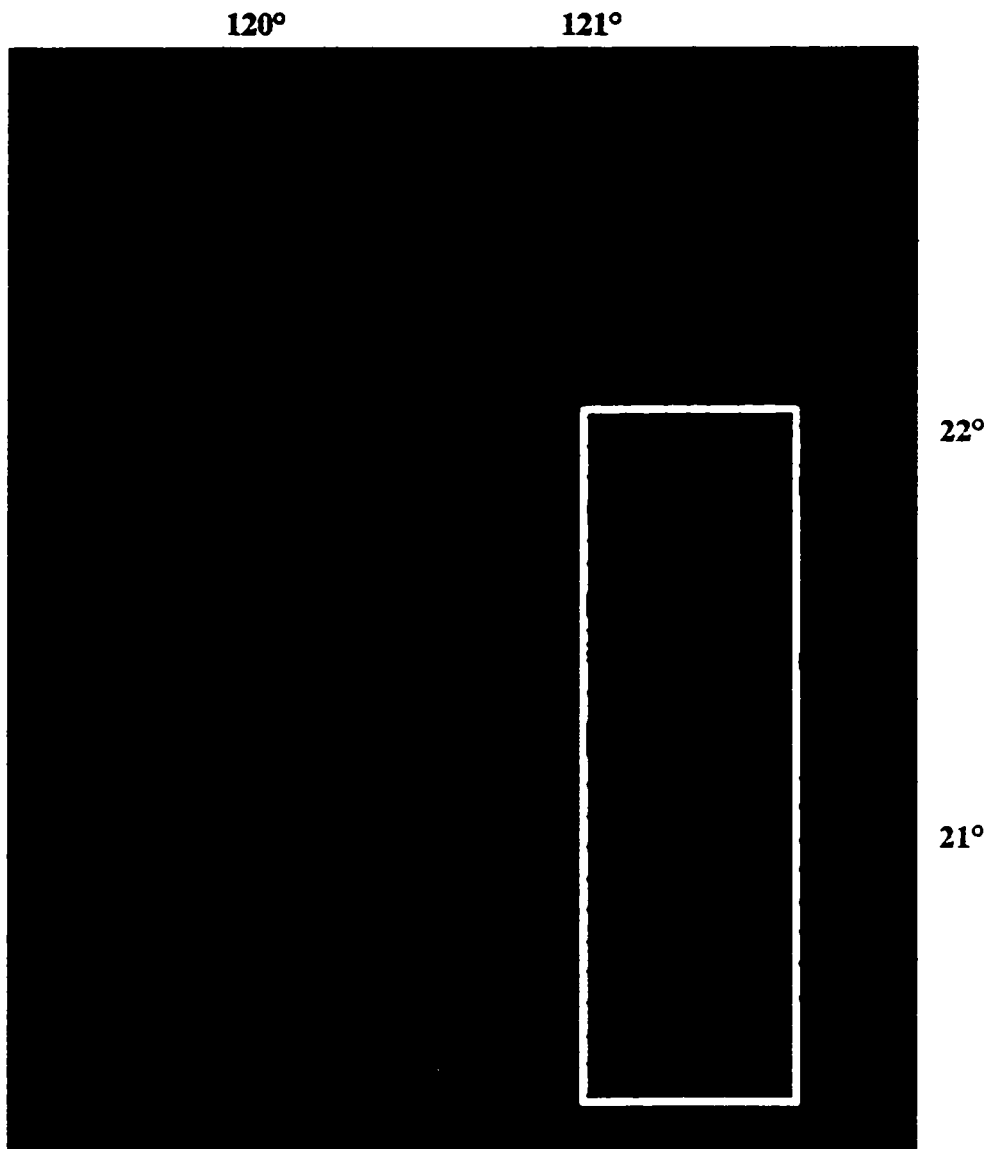


Figure 7. Map showing ship track lines for seismic survey MW-9006 (modified from Reed et al ., 1992). The white box indicates the outline of the study area.



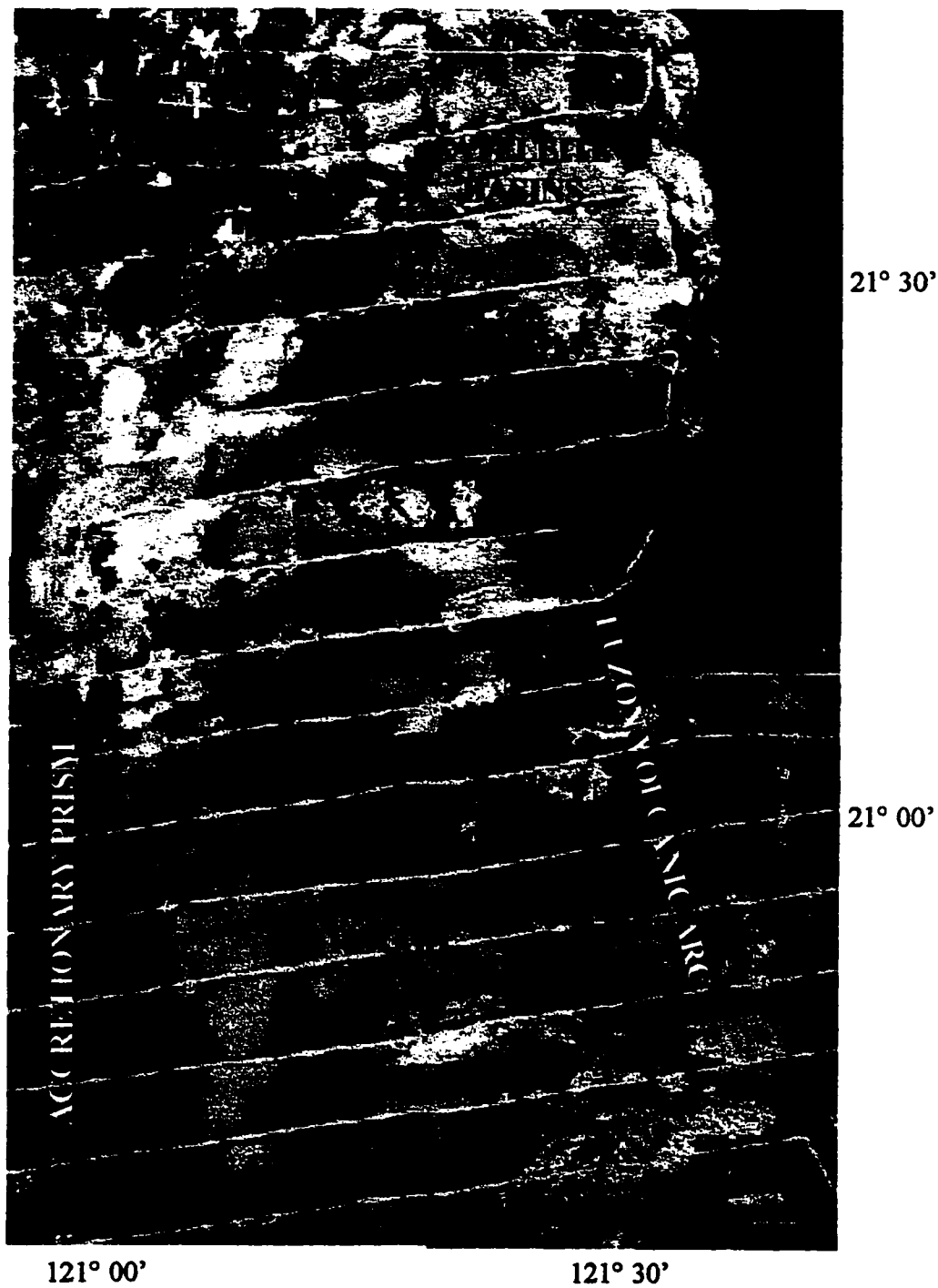


Figure 8. Portion of the side-scan sonar image mosaic showing the North Luzon trough study area. Dark areas denote high sonar backscattering and light areas are a result of low sonar backscattering.

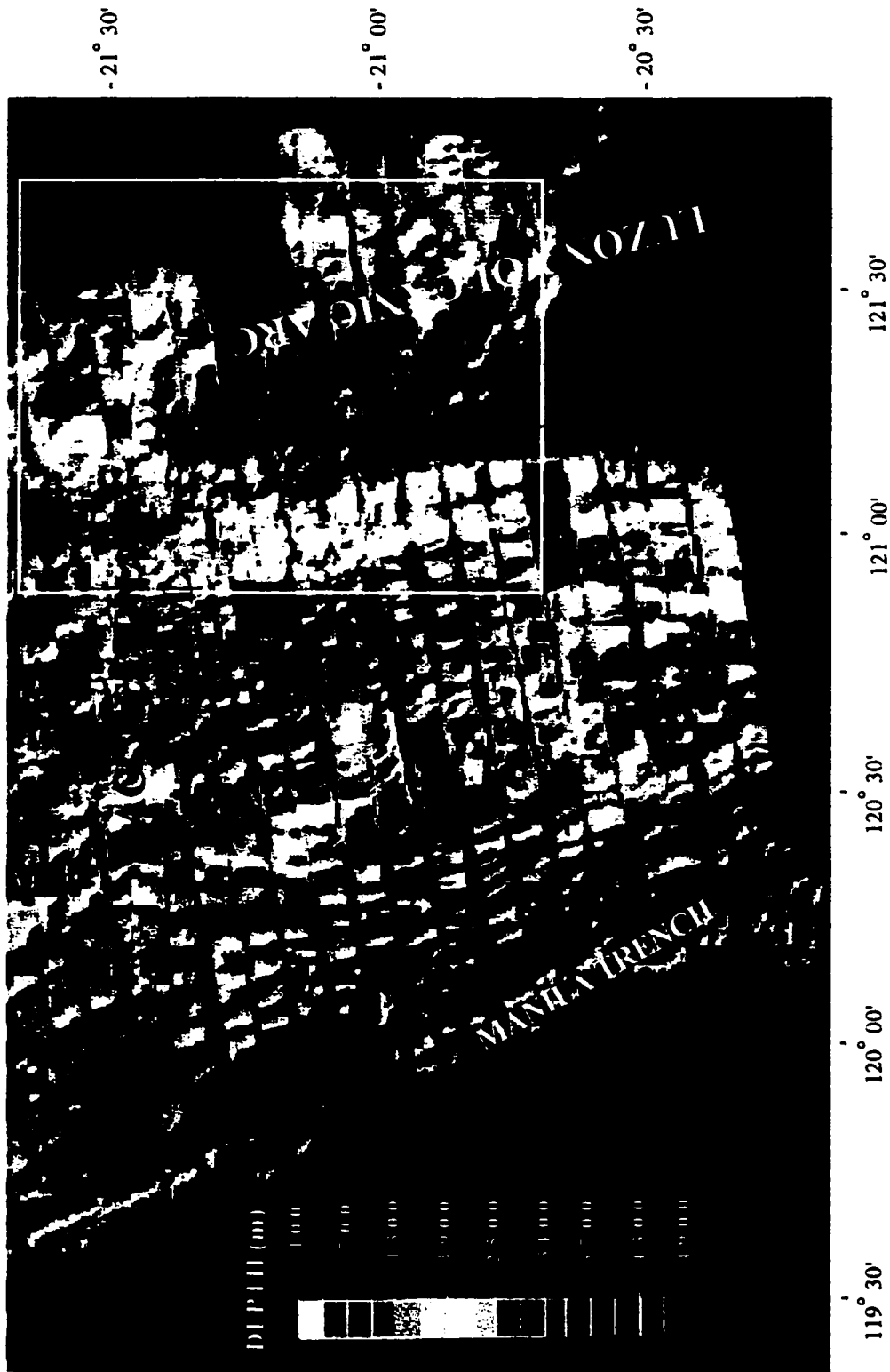


Figure 9. Map showing *SeaMARC II* bathymetric data of offshore southern Taiwan. The white box indicates the area shown in Figure 8.



**Figure 10. Seismic data processing flow used at University of California, Santa Cruz and San Jose State University.**

## DATA ANALYSIS

### Seismic Stratigraphy

#### Definition and Guidelines

One important aspect of this research involved the development of a stratigraphic framework for the North Luzon trough via seismic stratigraphic analysis. Seismic stratigraphy is the study of non-structural features of sedimentary rocks as interpreted from seismic data (Mitchum, 1977). This technique can be further subdivided into three sections: seismic sequence analysis, seismic facies analysis, and reflection character analysis.

Seismic sequence analysis involves identification of sequences, or groups of reflections, bounded by discontinuities within seismic sections. The discontinuities, or sequence boundaries, are the result of erosional or non-depositional events separating periods of relatively uniform sediment deposition.

The description and interpretation of reflection patterns is termed seismic facies analysis, and involves the recognition of reflection patterns that are characteristic of various types of depositional settings and processes.

Reflection character analysis is the study of lateral changes in individual reflections. These changes include aspects such as reflection continuity, amplitude, frequency, and waveshape.

## Geometry and Distribution of Sequences

The forearc basin is bounded by the Luzon volcanic arc to the east and the rear of the Taiwan offshore accretionary prism to the west (Fig. 5). North Luzon trough is broad and deep to the south, with sediments reaching approximately 4.0 sec (two-way travel time) in thickness. North of approximately  $20^{\circ} 45' N$ , the trough gradually becomes narrow and shallow and sedimentary sequences decrease in thickness. Figure 11 is an isochron map of total sediment thickness in the forearc basin illustrating this relationship.

The sediments of the basin were divided into nine sequences based on seismic facies and reflector strength characteristics (Fig. 12). Reflectors diverge to the east in the western region of the basin, are parallel within the center of the basin, and onlap the arc in the east with localized oblique characteristics; no major unconformities were identified in the central and eastern portions of the basin. Each sequence was mapped throughout the basin, and isochron maps of sequence thickness and depth to each sequence boundary were generated.

Sequence 9, the oldest sedimentary unit mapped in this study, overlies the eastern margin of the prism and the volcanic-arc basement to the east. It is narrow throughout the forearc basin as compared to the overlying sequences, and has a maximum observed thickness of approximately 0.72 sec (two-way travel time). This sequence, located south of approximately  $21^{\circ} 10' N$ , thins in an area near  $20^{\circ} 45' N$ , where it separates pockets of thick deposits in localized depressions in the volcanic arc topography. This sequence resembles a three-dimensional wedge thinning to the north and west. The westward

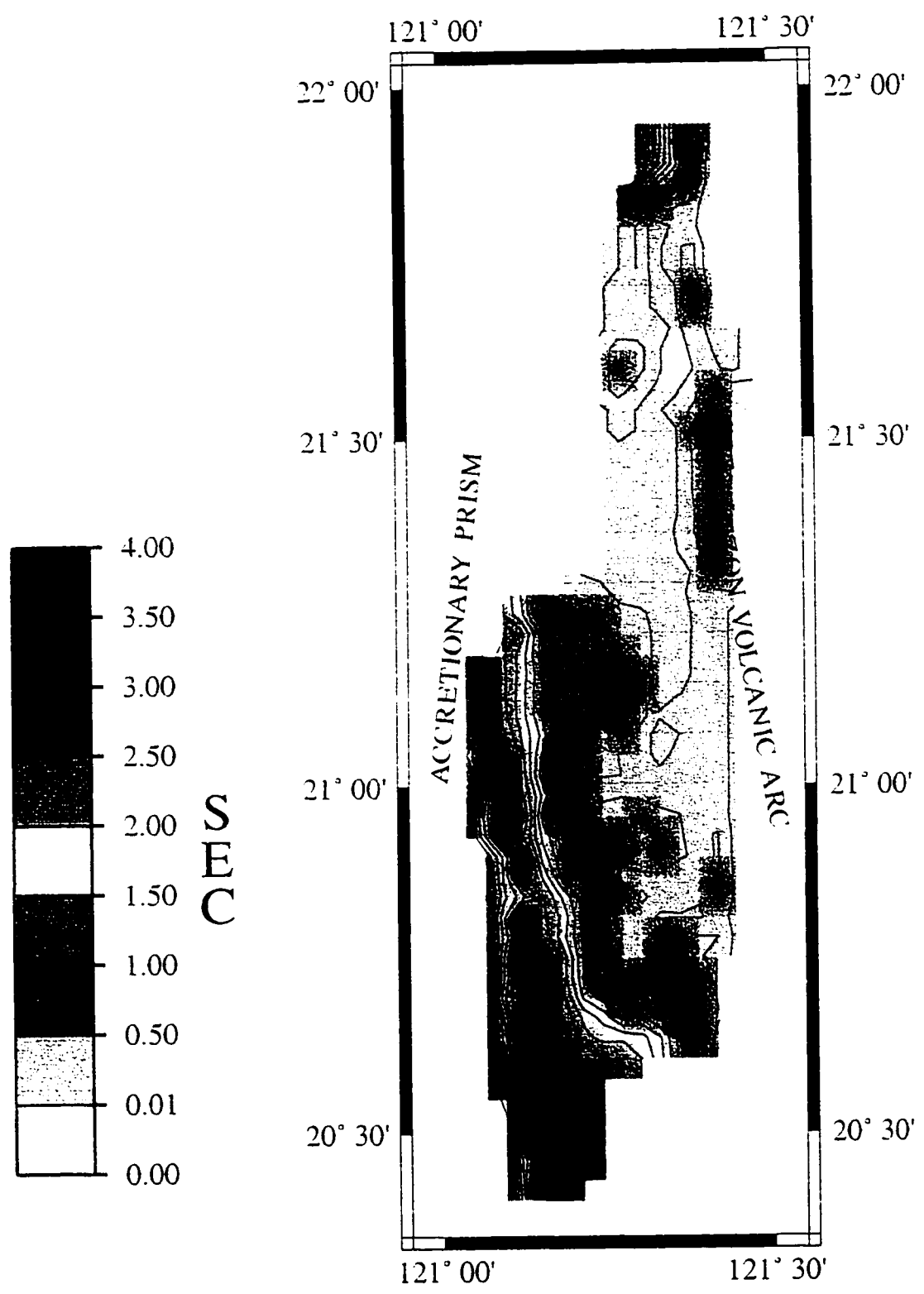


Figure 11: Isochron map of forearc basin sediment thickness in two-way travel time.

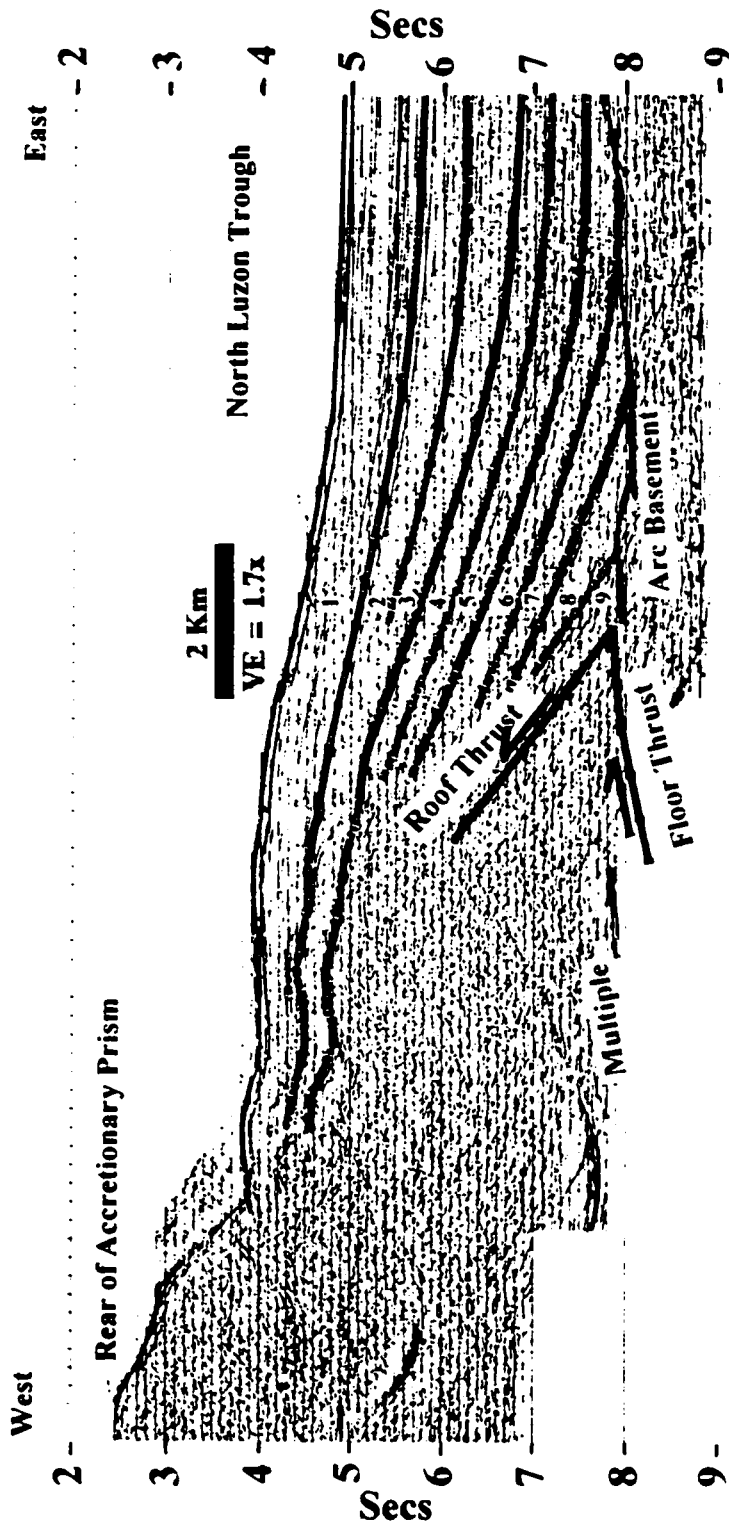


Figure 12. Cross-section of forearc basin sediments illustrating the division of stratigraphic sequences mapped throughout the North Luzon trough.

thinning of the sequence may reflect a component of tilting to the east due to uplift along the rear of the prism during the early history of the forearc basin.

Sequence 8 overlies sequence 9 and exhibits many of the same characteristics. It too is observed in seismic sections south of  $21^{\circ} 10' N$  and contains pockets of thin and thick deposits, though not as prominently as in sequence 9. The sequence thins near  $20^{\circ} 50' N$ , slightly north of the area of thinning of sequence 9. The sequence onlaps the volcanic-arc basement to the east and covers a broad region of the basin with a maximum thickness of approximately 0.58 sec (two-way travel time). The three-dimensional geometry is much the same as that of sequence 9, but there is a lesser degree of tilting in the west along the rear of the prism. The boundaries of this sequence are parallel in a west-east cross-sectional view of the basin.

Characteristics of sequence 7 include parallel reflectors and boundaries that onlap the volcanic arc farther to the east than the underlying sequences. The sequence covers a broader area than those underlying it, but is the thinnest of the nine sequences with a maximum thickness of 0.45 sec (two-way travel time). This sequence thins in an area between  $20^{\circ} 55' N$  and  $21^{\circ} 05' N$ . The sequence is wedge-shaped and decreases in thickness to the north and west.

Sequence 6 exhibits parallel internal reflectors and boundaries and is more extensive in the basin than previous sequences. The region of sequence thinning is present between  $20^{\circ} 55' N$  and  $21^{\circ} 00' N$ , but less pronounced as the sediments of this sequence



are more evenly distributed with a maximum thickness in the south of approximately 0.60 sec (two-way travel time).

Sequence 5 has the same reflector characteristics as sequence 6, but sequence 5 covers a slightly broader area, and has a maximum thickness of approximately 0.50 sec (two-way travel time). The region of sequence thinning is located near 21° 00' N and is more sharply delineated, compared with previous sequences. The sequence is wedge-shaped; however, this sequence is also present in a small satellite basin to the north between 21° 50' N and 22° 00' N.

Sequence 4 is also present in the satellite basin and is fairly uniform in the forearc basin with the exception of an area between 21° 05' N and 21° 10' N, where the thickness of the sequence reaches a maximum of approximately 0.70 sec (two-way travel time). The sequence is wedge-shaped and thins near 21° 00' N, with a gradual thickening to the north and south.

Sequence 3 marks a change in characteristics from the previous sequences. Its boundaries are parallel within the basin but converge to form a wedge-shaped body towards the western margin of the basin at the boundary with the accretionary prism. Reflectors in this area diverge to the east and gradually become more identifiable and parallel eastward. This sequence is present in satellite basins to the north, and contains localized areas of chaotic reflectors characteristic of slump deposits in the forearc basin north of 20° 45' N. The sequence thins between 20° 50' N to 20° 55' N and has a maximum thickness in the south of approximately 0.75 sec (two-way travel time).

Sequence 2 exhibits many of the same characteristics as sequence 3. The boundaries of this sequence are parallel in the east and converge near the western margin of the basin. As in sequence 3, the reflectors in the western region of the basin diverge to the east and become parallel eastward. This sequence is also present in the satellite basins to the north and contains regions of chaotic reflectors north of  $20^{\circ} 45' N$ . It thins from  $20^{\circ} 45' N$  to  $21^{\circ} 05' N$  and has a maximum thickness in the south of approximately 0.55 sec (two-way travel time).

Sequence 1 blankets the forearc basin and is the youngest of the nine sequences mapped. This sequence may be subdivided further, but the resolution of the data near the water bottom does not permit this due to ringing of the seafloor reflection. Thus, a maximum thickness of 1.45 sec (two-way travel time) for this sequence may be misleading. Even so, the general relationships observed remain the same. This sequence shows a thickness of  $>0.9$  sec (two-way travel time) in three distinct regions: the satellite basin to the north, an area around  $21^{\circ} 15' N$ , and in the region of the forearc basin south of  $20^{\circ} 35' N$ . Sequence 1 also exhibits the same wedge-shaped geometry as sequences 2 and 3. Reflector characteristics are also the same with eastward divergence of reflectors in the western edge of the basin gradually becoming parallel to the east. Areas of chaotic reflectors, marking slump deposits, were observed north of  $20^{\circ} 45' N$ ; a region of sequence thinning was observed between approximately  $20^{\circ} 50' N$  and  $21^{\circ} 00' N$ .

All sequences have been locally folded into broad anticlines between  $20^{\circ} 35' N$  and  $21^{\circ} 00' N$  (lines 44-39) and near  $21^{\circ} 20' N$  (line 18) (Fig. 13).

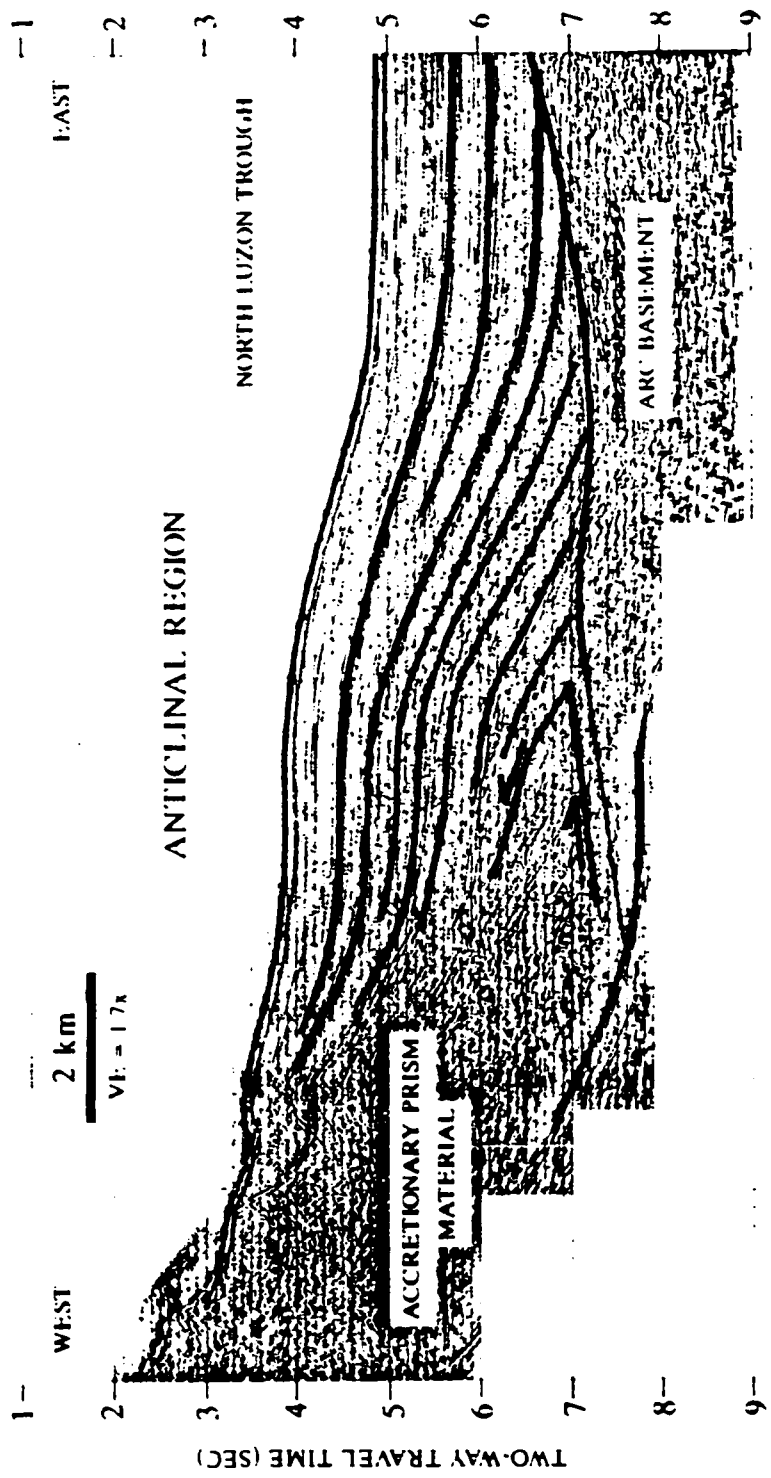


Figure 13. Cross-section of the forearc basin (line 20) illustrating broad anticline observed in sequences between 20° 35' N and 21° 00' N and near 21° 20' N.

### Sedimentary Processes

Observations regarding modern sedimentary processes active in the forearc basin were based on the analyses of *SeaMARC II* side-scan sonar and bathymetry data in the form of image mosaics. These mosaics show evidence of various types of deposits, including those formed by mass wasting and deposition of fan sediments throughout the forearc basin. Surficial evidence for mass wasting primarily along the western margin of the forearc basin is the presence of broad lobe deposits in the south that become more localized and abundant northward. North of 21° 00' N, towards the zone of collision, areas of high back-scatter on the side-scan sonar image associated with mass wasting processes appear more abundant. These deposits become more evident northward. This suggests an increase in the frequency of these depositional events in this tectonic setting. Submarine canyons along the rear of the accretionary prism tend to promote mass wasting near 21° 15' N. Presumably, canyon development in this area is a result of a rapid change in topography from the flat seafloor of the forearc basin to the steep slope above the backthrust domain of the accretionary prism, coupled with the close proximity of the area of basin closure. Although submarine canyons with associated fan deposits are identifiable along both margins of the basin, they are more abundant along the western flank of the Luzon volcanic arc. The submarine canyons on the volcanic arc are well-developed and distribute sediments to the basin forming a pattern characteristic of a fan. Localized debris-flow deposits, not always associated with submarine canyons, also were identified along the eastern margin of the basin. These deposits appear smaller than the broad lobes of sediment on the western margin of the basin. In addition to surficial sedimentary

deposits, the mosaics also show features that affect sediment flow into the forearc basin. These features include bathymetric highs and submarine canyons in the north where closure of the forearc basin has cut off or diverted sediment away from the forearc basin, through the island arc, and into the backarc region. In some cases, the bathymetric highs have resulted in the creation of satellite basins that prevent sediments from entering the North Luzon trough to the south. The cumulative effect of such features is a significant decrease in the sedimentation rate within the forearc basin following the onset of collision.

## INTERPRETATIONS

### Seismic Stratigraphy

The seismic stratigraphic framework for the North Luzon trough can be used to study patterns of uplift and the source of sediments within the forearc region. The lower sequences, sequences 4 through 9, can be grouped together due to the parallel relationship of their reflectors and sequence boundaries. Sequences 8 and 9 are the deepest sequences in the forearc basin and therefore represent the earliest deposited sediments at a time when the accretionary prism was first beginning to form along the Manila trench. Both sequences lap onto the rear of the accretionary prism and have been uplifted and tilted during the initial formation of the accretionary prism. The parallel relationship of reflectors and boundaries in sequences 4 through 7 suggest periods of relatively uniform sedimentation and little or no uplift. During this period, the depositional processes affecting forearc basin strata were dominated by broad sheet flows dispersing sediment widely throughout the basin with the island of Taiwan as the dominant sediment source. Many of these flows may have traveled southward along the axis of the forearc basin and coalesced with other sheet flow deposits, thus producing basinwide sheet deposits.

In contrast to the parallel reflectors and sequence boundaries of sequences 4 through 7, the upper three sequences show a convergence of their boundaries to the west. This observation, along with the presence of diverging reflectors at the boundary with the prism and areas of chaotic reflectors characteristic of slump deposits, suggests that the

area has experienced a recent period of uplift. Thus, the boundary between sequence 3 and sequence 4 can be interpreted as the time of onset of uplift. Sequence boundary relations could be used to accurately date the onset of basin closure if ODP drilling were to take place. The inferred uplift is presumably the result of tectonic wedging that was first proposed in this region by Reed et al. (1992). This process involves a wedge of accretionary prism material moving eastward beneath the basin sequences via a floor and roof thrust system, which lifts the western edge of the sequences as they move along the roof thrust of the wedge (Fig. 14). The roof thrust is eventually cut at shallower depths by backthrusting along east-vergent thrusts, resulting in the incorporation of forearc basin sediments into the rear of the accretionary prism. Once incorporated, the sediments are subjected to uplift on the order of 1000m as the tectonic wedge migrates eastward. The uplifted region has produced extensive debris-flow deposits along the floor of the North Luzon trough extending eastward from steep slopes along the rear of the accretionary prism. Hence, uplifted sediments become unstable and subject to processes of mass wasting on slopes greater than  $15^{\circ}$ . These processes may be triggered in several ways, but the primary catalyst may be seismicity in the region.

The most recognizable of the recent sedimentary deposits within the forearc basin are slumps and localized arc-fan debris-flow deposits. Mass wasting of sediments indicated by chaotic reflectors in seismic profiles is evident from approximately  $20^{\circ} 55' N$  to  $21^{\circ} 15' N$ . This is most apparent on lines 19 and 20 where chaotic reflectors are present from the water-bottom through sequence 3. This suggests an ongoing period of

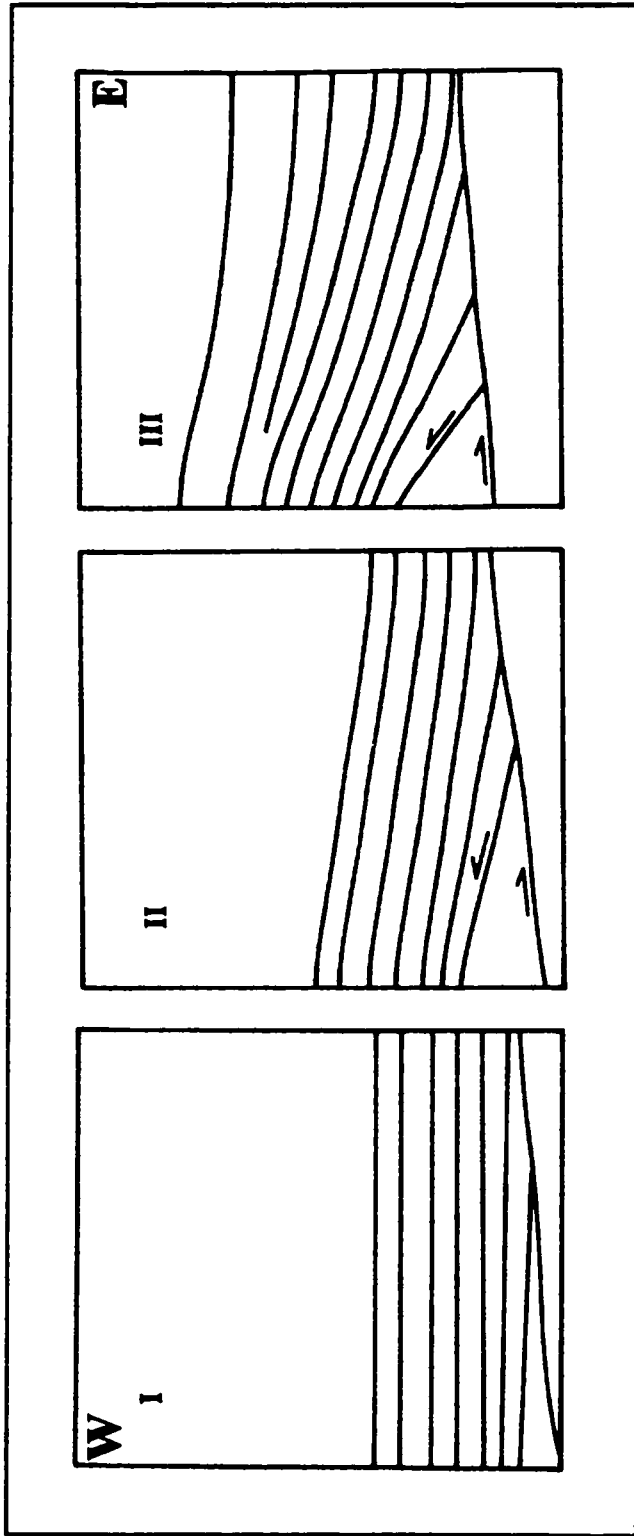


Figure 14. Model illustrating the eastward progression of the tectonic wedge with time: (I) deposition of flat-lying sequences; (II) initial uplift; (III) continuing uplift resulting in wedge-shaped deposits of ongoing sedimentation.



uplift and slumping along the rear of the prism in this northern region of the forearc basin. In fact, isochron maps of every sequence show evidence for increased deposition in the northern region of the basin where modern slumping is widespread. In the lower sequences, this region of thickening could be attributed to terrigenous sediments from Taiwan before the closure of the basin and to minimal debris-flow deposits derived from the offshore accretionary prism and the Luzon volcanic arc. However, as the arc-continent collision closed off the forearc basin, the primary depositional mode changed to mass wasting of accretionary prism material and debris flows from the volcanic arc.

The lack of major unconformities and parallelism of reflectors in forearc basin strata suggest the absence of significant tilting or flexure of the volcanic-arc basement. Consequently, thrust loading caused by backthrusting appears to be minor to absent. However, the topography of the volcanic arc has had a significant influence on the basin sediments. The broad anticlines in seismic sequences, observed between approximately  $20^{\circ} 35' N$  and  $21^{\circ} 00' N$  (lines 44-39) and also near  $21^{\circ} 20' N$  (line 18), correspond to localized areas of steep volcanic-arc basement topography within the forearc basin (Fig. 15). This steep topography is likely a remnant of a small seamount in the arc basement that provides a back-stop for basin sediments. A broad anticline in the basin strata has formed where the western slope of the seamount has been thrust beneath the eastward advancing tectonic wedge of Taiwan's offshore accretionary prism (Fig. 13).

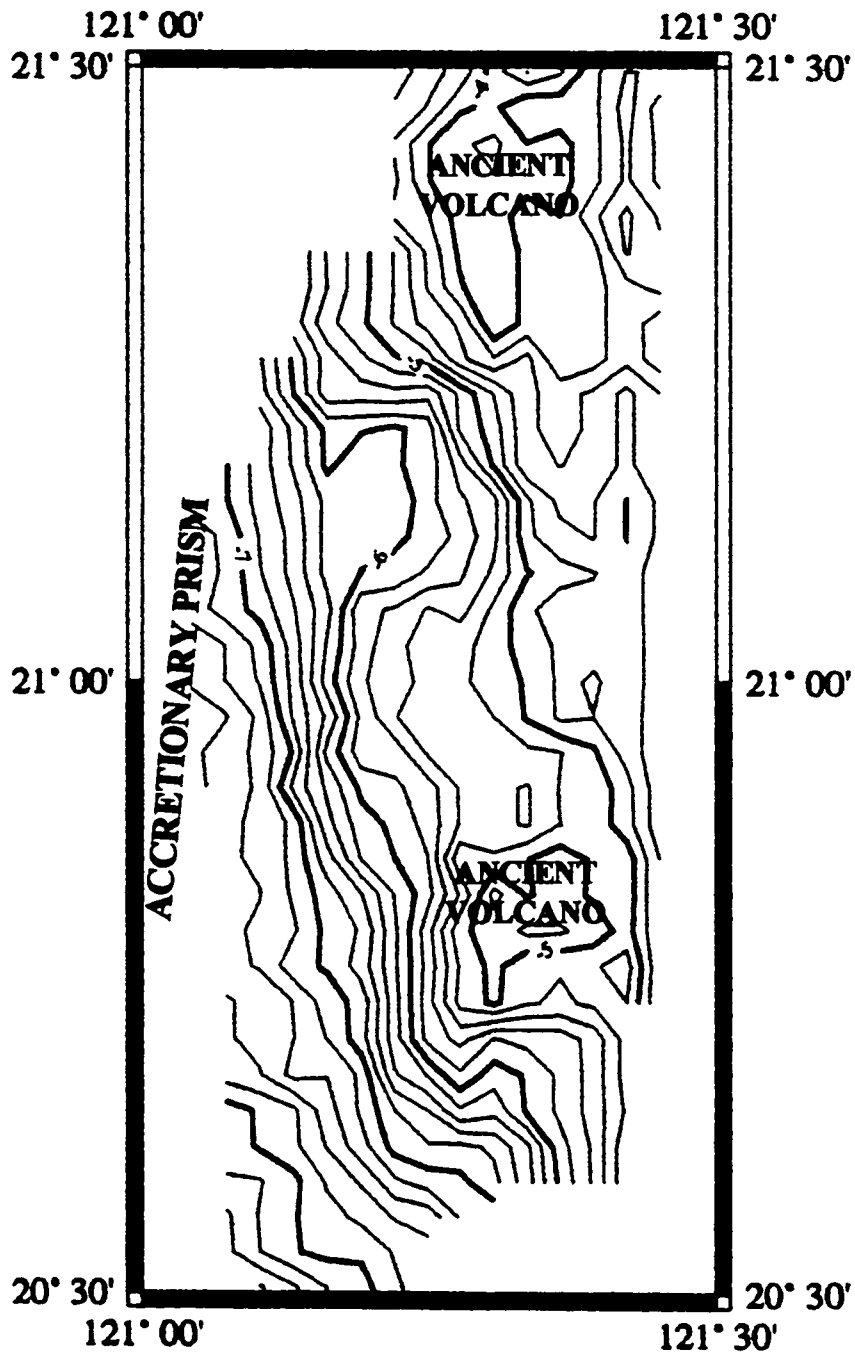


Figure 15. Two-way travel time contour map of a portion of the volcanic arc basement underlying the forearc basin sediments showing steep topography likely due to ancient volcanoes.

### Sedimentary Processes

The primary sources of sediment in the North Luzon trough include Taiwan's offshore accretionary prism to the west, the Luzon volcanic arc to the east, and the island of Taiwan to the northwest. Cores taken in the forearc basin reveal sediment dominated by quartzolitic turbidite sands interbedded with hemipelagic mud, coarse arc detritus, and occasional volcanic ash beds (Lundberg et al., 1995). Figure 16 shows the author's interpretation of surficial sediment in the forearc basin using the *SeaMARC II* side-scan sonar mosaic. All three of the primary sediment sources have played an important role in contributing to the sediment budget of the North Luzon trough at one time or another. Sequences 9 through 4 were likely to have been deposited during a period when all of the primary sources contributed sediment to the forearc basin. Sequences 3 to 1 most likely contain sediments from the primary sources with a decrease in contributions from the Taiwan orogen throughout the transition of forearc basin closure. In addition to the sediment trap created by the Southern Longitudinal trough, bathymetric highs form prominent barriers as a result of the impingement of the Luzon volcanic arc onto the rear of Taiwan's offshore accretionary prism. This closure of the northern margin of the forearc basin effectively cuts off the sediment pathways from the island of Taiwan and the Southern Longitudinal trough. In addition, the juxtapositioning of the Luzon volcanic arc topography to the rear of the accretionary prism creates smaller satellite basins north of the forearc basin that serve as sediment traps, blocking the southward flow of detritus. Thus, closure of the basin has resulted in significant reduction of sediment introduced into

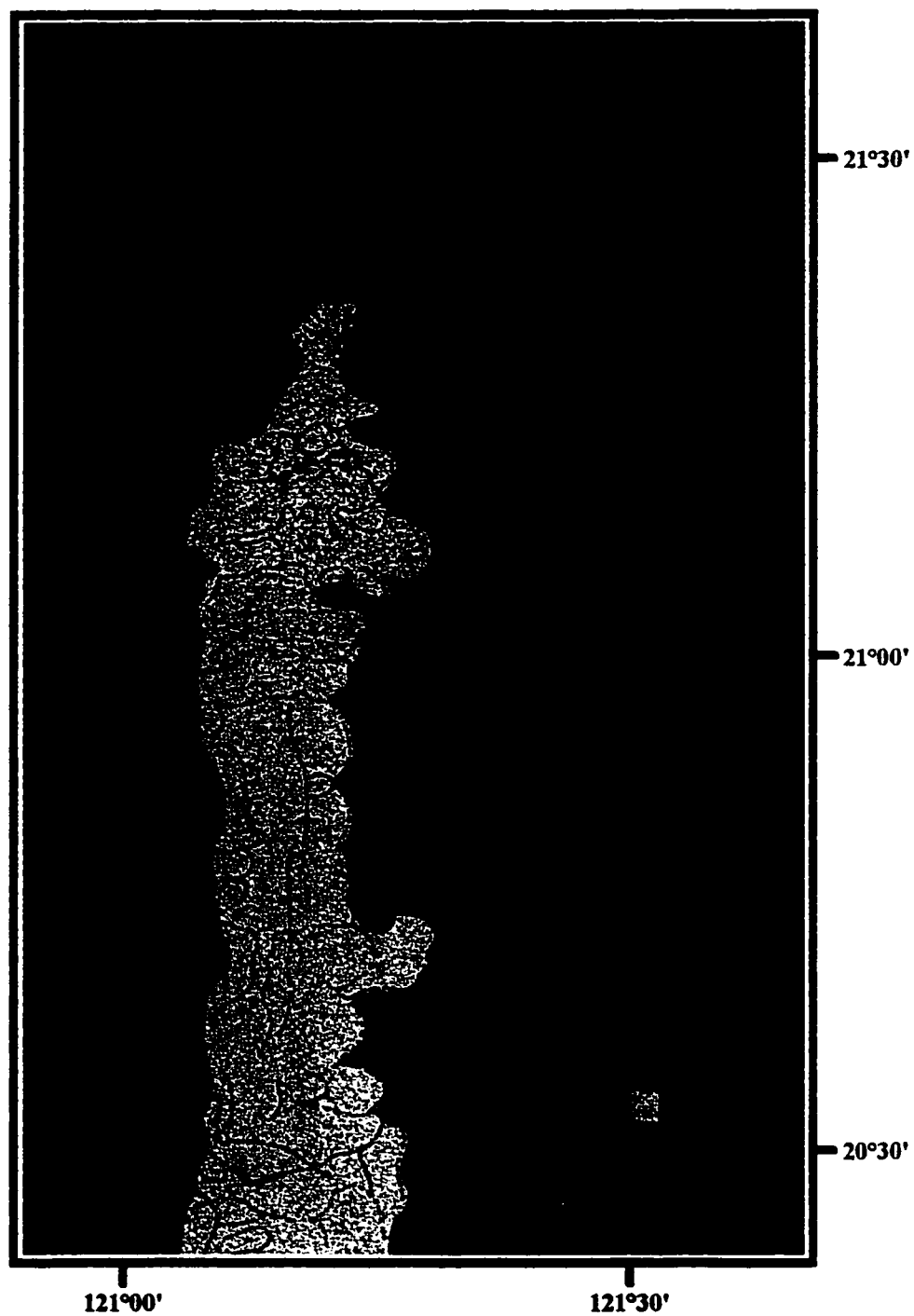


Figure 16. Side-scan sonar interpretation of surficial sediment within the North Luzon trough.

the North Luzon trough. The amount of sediments derived from the island of Taiwan is also affected by a large submarine canyon north of the Southern Longitudinal trough at approximately 22° 25' N (Fig. 17). This canyon diverts sediment away from the Southern Longitudinal trough, the satellite basins, and consequently the North Luzon trough into the backarc region of the subduction complex.

The closure of the forearc basin marks a change in sedimentation and depositional processes. In its early stages, sediment was dispersed throughout the basin in a relatively uniform manner, with the island of Taiwan serving as the primary source of sediment. After the impingement of the Luzon volcanic arc to the rear of the accretionary prism and subsequent uplift of basin strata, mass wasting of the accretionary prism became the dominant process.

Following basin closure, detritus carried to the forearc basin have been derived from the Luzon volcanic arc to the east and the accretionary prism to the west. The *SeaMARC II* side-scan sonar mosaic shows the buildup of recent fan and debris-flow deposits originating from the western flank of the Luzon volcanic arc. Distribution of arc-derived sediment is, for the most part, related to the bathymetric highs of the Luzon volcanic arc. The fan deposits are located at the mouths of numerous submarine canyons which channel sediment through the volcanic arc topography. Debris-flow deposits (Fig. 18) occur most commonly along the base of the steeper inclines of the accretionary prism and the volcanic arc.

A substantial source of sediments for the basin comes from Taiwan's offshore accretionary prism. The *SeaMARC II* data show evidence of mass wasting of accretionary

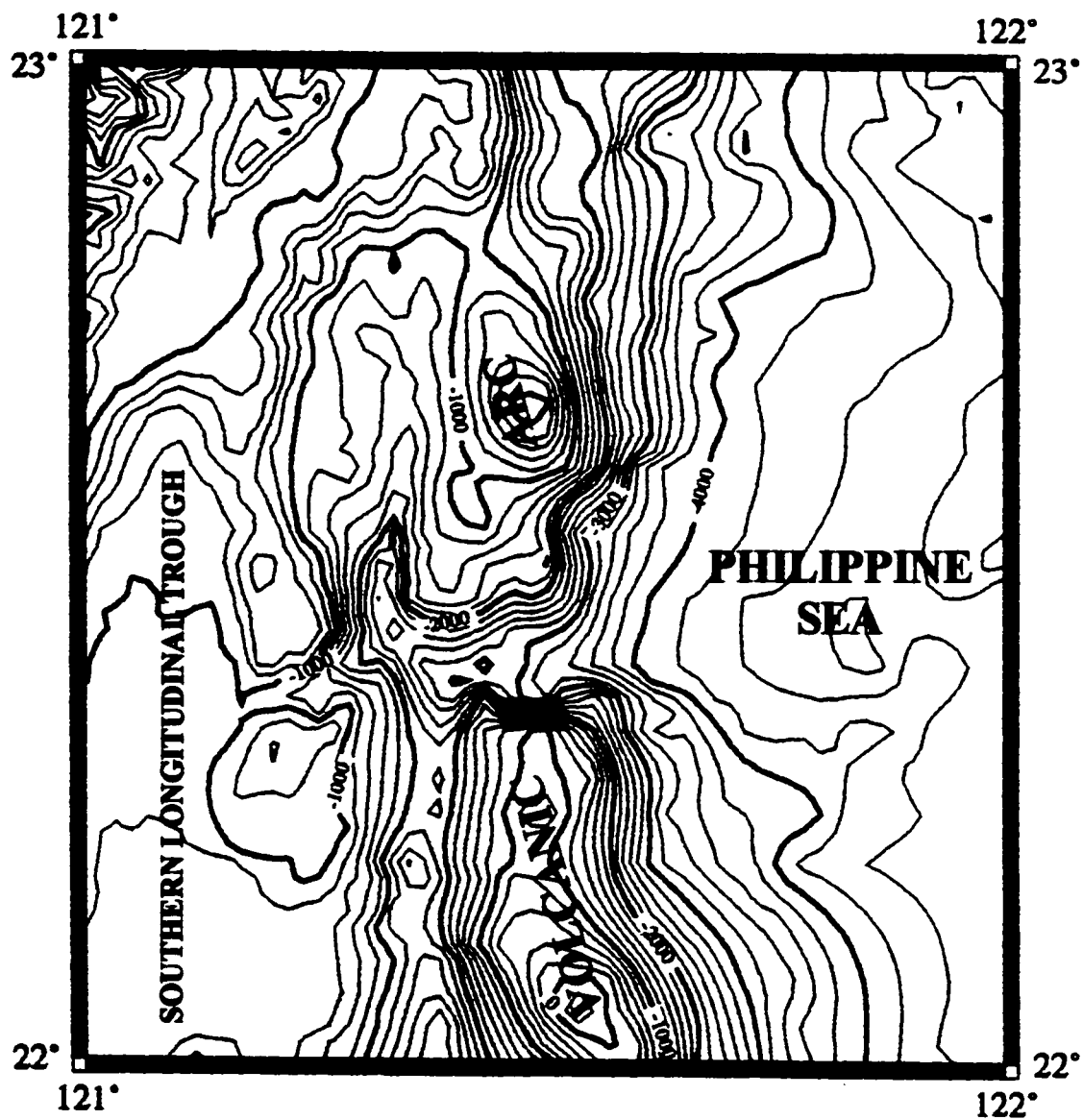


Figure 17. Contour map showing the submarine canyon north of the forearc basin which diverts sediment towards the backarc region.

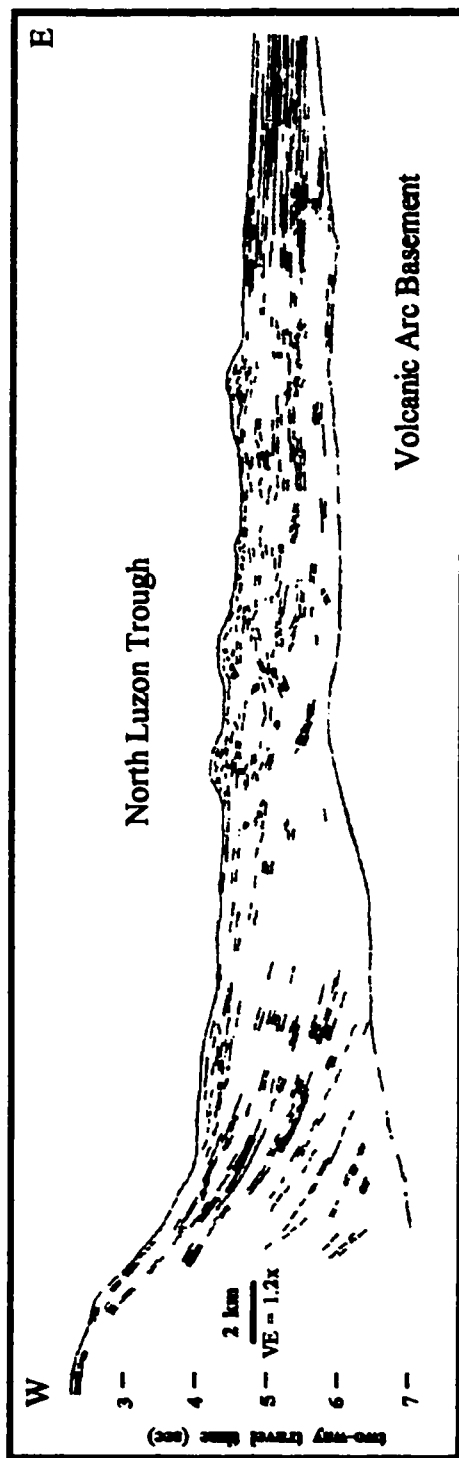


Figure 18. Drawing of line 20 showing evidence for debris-flow deposits within the forearc basin in the form of chaotic reflectors and surface irregularities.

prism sediments in the form of debris-flow deposits all along the western margin of the North Luzon trough (Fig. 19). This mass wasting is the result of a series of events including the incorporation of forearc basin sediments into the rear of the accretionary prism due to backthrusting, uplift of these sediments as a result of tectonic wedging, and the eventual redeposition of the sediments into the basin in the form of mass wasting. This process is continually repeated, resulting in significant recycling of sediments of the forearc basin. Material accreted early along the Manila trench and orogenic detritus derived from the island of Taiwan and deposited in the forearc basin also may be involved in this process. Apart from fundamental deep-marine sedimentary processes, such as the deposition of sediments suspended in the water column, deposition in the modern forearc basin is dominated by mass wasting in the form of sediment-gravity flows. These processes result in the deposition of broad sheet deposits distributed throughout the basin. This may be attributed to turbidity currents which can develop sheet-like bodies tens of kilometers wide (Shanmugam and Moiola, 1991). In addition, possible reworking or redistribution of sediment within the forearc basin may be due to bottom currents.



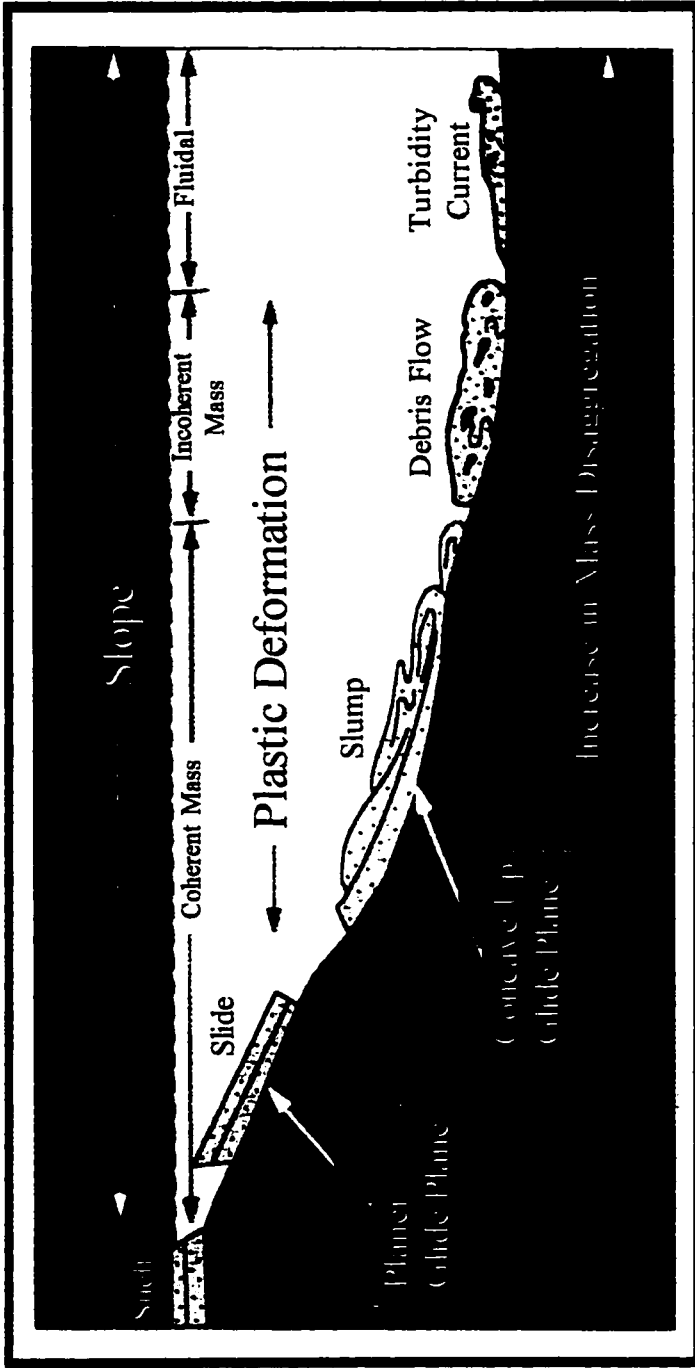


Figure 19. Model showing progressive forms of mass wasting from slide to turbidity current (modified from Shanmugam et al., 1994).

## CONCLUSIONS

The boundary between sequence 3 and sequence 4 is significant for dating the timing of uplift of forearc basin sediments due to backthrusting along the rear of Taiwan's offshore accretionary prism. This backthrusting, coupled with the eastward migration of a tectonic wedge beneath forearc basin sediments, has resulted in multiple cycles of uplift and mass wasting of sediments within the North Luzon trough. Major sedimentary processes in the modern forearc basin include mass wasting of material from the rear of the offshore accretionary prism and the formation of debris-flow and arc-fan deposits from the western flank of the Luzon volcanic arc. Evidence of these processes is not observed in older, basin-fill sequences of the forearc basin indicating a change from the deposition of basin-wide turbidites derived from the Taiwan orogen to localized sedimentary deposits derived from the rear of the accretionary prism and the volcanic arc. This shift in sedimentation marks the time of forearc basin closure, leading to the creation of satellite basins to the north that serve as traps for sediment derived from Taiwan thereby preserving evidence for the onset of collision in the region.

## REFERENCES

- Angelier, J., Bergerat, F., Chu, H. T., and Lee, T. Q., 1990, Tectonic analysis and the evolution of a curved collision belt: the Hsuehshan Range, northern Taiwan: *Tectonophysics*, v. 183, p. 77-96.
- Beaudry, D. and Moore, G. F., 1985, Seismic stratigraphy and Cenozoic evolution of west Sumatra Forearc Basin: *American Association of Petroleum Geologists Bulletin*, v.69, p. 742-759.
- Beer, J. A., Allmendinger, R. W., Figueroa, D. E., and Jordan, T. E., 1990, Seismic stratigraphy of a Neogene piggyback basin, Argentina: *American Association of Petroleum Geologists Bulletin*, v. 74, p. 1183-1202.
- Lewis, S. D., and Hayes, D. E., 1984, A geophysical study of the Manila Trench, Luzon, Philippines 2. Forearc basin structural and stratigraphic evolution: *Journal of Geophysical Research*, v. 89, p. 9196-9214.
- Lundberg, N., and Dorsey, R. J., 1988, Synorogenic subsidence and sedimentation in a Plio-Pleistocene collisional basin, eastern Taiwan: *in* Kleinspehn, K. L. and Paola, C., eds., *New perspectives in basin analysis*: New York, Springer-Verlag, p. 265-280.
- Lundberg, N., Reed, D. L., Liu, C.-S., Chen, M.-P., and Gerace, D. A., 1995, Forearc-basin closure and orogenic sedimentation in the submarine suture zone south of Taiwan: Response to arcward transfer of plate convergence: *in* Tsien, H. H., ed., *International conference and third Sino-French symposium on active collision in Taiwan; Programs and Extended Abstracts*: Geological Society of China, p. 243-247.
- Mitchum, R. M., Vail, P. R., and Thompson, S., 1977, The depositional sequence as a basic unit for stratigraphic analysis, *in* Payton, C. E., ed., *Seismic stratigraphy - applications to hydrocarbon exploration*: American Association of Petroleum Geologists, Memoir 26, p. 53-62.

- Mitchum, R. M., 1977, Glossary of terms used in seismic stratigraphy, *in* Payton, C. E., ed., *Seismic stratigraphy - applications to hydrocarbon exploration*: American Association of Petroleum Geologists, Memoir 26, p. 205-212.
- Ori, G. G., and Friend, P. F., 1984, Sedimentary basins formed and carried piggyback on active thrust sheets: *Geology*, v. 12, p. 475-478.
- Price, R., 1986, The southeastern Canadian Cordillera: thrust faulting, tectonic wedging, and delamination of the lithosphere: *Journal of Structural Geology*, v. 8, p. 239-254.
- Reed, D. L., Lundberg, N., Liu, C.-S., and Kuo, B. Y., 1992, Structural relations along the margins of the offshore Taiwan accretionary wedge: implications for accretion and crustal kinematics: *ACTA Geologica Taiwanica*, no. 30, p. 105-122.
- Seno, T., 1977, The instantaneous rotation vector of the Philippine Sea plate relative to the Eurasian plate: *Tectonophysics*, v. 42, p. 209-226.
- Shanmugam, G., Lehtonen, L. R., Straume, T., Syvertsen, S. E., Hodgkinson, R. J., and Skibeli, M., 1994, Slump and debris-flow dominated upper slope facies in the Cretaceous of the Norwegian and northern North seas (61-67°N): Implications for sand distribution: *American Association of Petroleum Geologists Bulletin*, v. 78, p. 910-937.
- Shanmugam, G., and Moiola, R. J., 1991, Types of submarine fan lobes: models and implications: *American Association of Petroleum Geologists Bulletin*, v. 75, p. 156-179.
- Silver, E. A., and Reed, D. L., 1988, Backthrusting in accretionary wedges: *Journal of Geophysical Research*, v. 93, p. 3116-3126.
- Speed, R. C., Torrini, R., and Smith, P. L., 1989, Tectonic evolution of the Tobago Trough forearc basin: *Journal of Geophysical Research*, v. 94, p. 2913-2936.

- Suppe, J., 1984, Kinematics of arc-continent collision, flipping of subduction, and back-arc spreading near Taiwan: *Memoir of the Geological Society of China*, no. 6, p. 21-33.
- Teng, L. S., 1991, Geology of Taiwan in the tectonic framework of arc-continent collision: *Taicrost Workshop Proceedings*, Institute of Oceanography, National Taiwan University, Taipei, ROC, p. 63-74.
- Torrini, R., and Speed, R. C., 1989, Tectonic wedging in the forearc basin-accretionary prism transition, Lesser Antilles forearc: *Journal of Geophysical Research*, v. 94, p. 10549-10584.
- Unruh, J. R., Ramirez, V. R., Phipps, S. P. and Moores, E. M., 1991, Tectonic wedging beneath forearc basins: Ancient and modern examples from California and the Lesser Antilles: *Geological Society of America Today*, v. 1, p. 185-190.